

Study of Graphite DC Arc for Preparing Carbon Nanotubes

Zuhoor Elahi^{a*}, Shahid Mahmood^a and Muhammad Zakauallah^b

^aDepartment of Physics, University of Karachi, Karachi, Pakistan

^bRafi Chaudhry Chair, Centre for Advanced Studies in Physics, GC University,
1 Church Road, Lahore-54000, Pakistan

(received November 8, 2021; revised August 23, 2022; accepted August 23, 2022)

Abstract. The production of carbon nanotubes is investigated using a graphite DC Arc plasma column. The goal was to look into the experimental variables that influence the creation of nano-structures. The intensities of consecutive ionization stages in the line spectrum are used to calculate excitation temperatures. The excitation temperature and delay time have been calculated and found to have an exponential relationship. Electron densities in the arc plasma are also calculated for various times and found to be falling exponentially as the plasma cools down. Carbon nanotubes generated during the arc are collected as soot from the cathode and analysed for their shape, content and structural characteristics. The nanotubes that are generated are found to be multi-walled in nature.

Keywords: DC Arc, carbon nanotubes, excitation temperature, electron density

Introduction

Nanotechnology has made it possible to use nanoparticles smaller than 100 nanometers in a variety of applications. Nanoparticles are used in a variety of applications and researchers are constantly looking for new ways to use them. Following the discovery of carbon nanotubes, researchers have been working to develop efficient synthesis methods. However, there hasn't been much published study on the fundamental techniques that occur in the graphite arc where these structures grow. The study of graphite arc plasma is necessary to comprehend the synthesis and decay of carbon molecules in a high temperature environment, which is linked to the formation of carbon nano-structures. Optical emission spectroscopy seems to be a particularly suitable approach for these kinds of investigations. There have already been some fairly good results on the properties of carbon plasma in the fabrication of carbon nano-structures. The formation of carbon nanotubes in a DC/AC arc between graphite terminals occurs in a chaotic environment that is difficult to manage on such a small scale. On the other hand, many tactics for modifying the arc discharge can be predicted on a large scale, such as pressure, input voltage/current regulation, distance between the electrodes, electrode diameters, or adjusting condensation rates using various cooling approaches. (Iijima, 1991)

*Author for correspondence;

E-mail: zuhoor.elahi@uok.edu.pk

Carbon nanotubes can be used as a catalyst medium in a fuel cell, avoiding the use of platinum, which is quite expensive and is used in most catalysts. Several researchers have devised a method for creating integrated circuits using carbon nanotubes. Researchers have established a method for connecting multi-walled carbon nanotubes to the metallic pads of integrated circuits without the significant interface resistance created by conventional manufacturing processes by using a new technique for precisely controlling the deposition of carbon (Physics.org, 2012). Arc discharge was the first method for making single walled nanotubes that was widely accepted (SWNTs) (Aabir *et al.*, 2022; Arora and Sharma, 2014; Bethune *et al.*, 1993; Iijima and Ichihashi, 1993) and multi walled nanotubes (MWNTs) (Iijima, 1991). Krätschmer *et al.* (1990) used the graphite bars in contact by applying an AC voltage in a noble gas environment to create Bucky balls, while in the DC arc the positive anode is sublimated and creates fullerenes (Saito *et al.*, 1992) as ash in the chamber and a small amount of the positive electrode is dissipated and stored on the negative electrode in the form of powder. In that cathode deposit, Iijima (1991), first observed the carbon nanotubes. The yield for this approach is dependent upon 30% by weight. In this approach, both SWNTs and MWNTs are formed with their lengths up to 50 micrometers (Collins *et al.*, 2000). The temperature of the carbon arc is also a crucial factor in defining the properties of carbon nanotubes. To comprehend the

formation of carbon nanomaterial, precise temperature measurement is essential. The excitation temperature, however, cannot be determined using traditional methods due to the arc's tremendous radiation and dynamic behaviour.

In the present work, we have used the Boltzmann plots to solve the above problem in measuring the temperature (Kolesnikov *et al.*, 2018), while the electron density is calculated using the Saha-Eggert relationship (Safi *et al.*, 2019). The objective of this work is to measure the excitation temperature and the electron density, during the arc discharge. The morphological, elemental and structural analyses are also performed.

Materials and Methods

The experimental setup is shown in Fig. 1. A small stainless steel vacuum chamber, which is shown in Figs. 1(a-d) is used for the formation of DC arc between the graphite electrodes. The schematic diagram with dimensions is in the Fig. 1(e). The complete setup is shown in the Fig. 1(f). The deposition chamber consists of five major components; the chamber, sample holders, optical window, the vacuum system and two electrodes, which are connected to the external power supply. The chamber has four ports on two perpendicular axes. The inner diameter of the viewing ports is 3 cm. Two ports are used as feed through for the electrodes, one port for

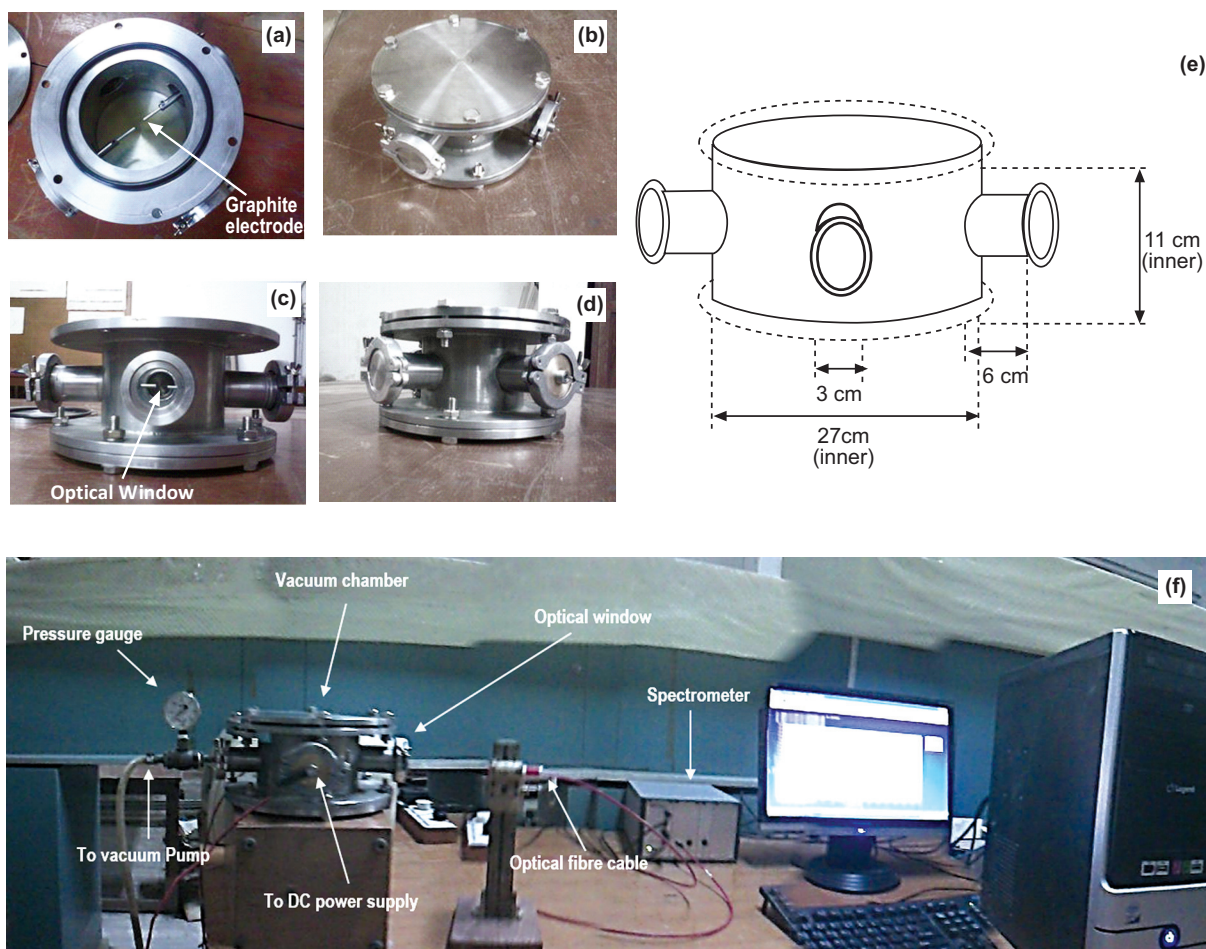


Fig. 1. A stainless-steel vacuum chamber used for the development of the dc arc plasma. **(a)** Inside view of the chamber showing the graphite electrodes. **(b)** Top view of the chamber. **(c)** Optical (quartz) window. **(d)** Side view of the chamber. **(e)** Schematic of the chamber showing the inner and outer dimensions of the chamber and the tubes. **(f)** The complete experimental setup consisting of the vacuum chamber connected to a vacuum pump, a spectrometer (Avantes, ava-spec (2048)) attached with the chamber window through optical fibre cable and a computer system to record the spectra.

gas inlet/outlet and one for the collection of light signals from the plasma (quartz window). A spectrometer (Avantes, ava-spec (2048)) is attached with the chamber window through optical fibre cable. The temperature of the electrodes can be adjusted for different values of current as it is an important factor which the properties of the produced nanoparticles depend on.

During the arc, carbon nanotubes are formed. Optical studies of the arc during the formation of carbon nanotubes are carried out by Avantes spectrometer (Avantes; AvaSpec-2048 StarLine; 360 nm to 860 nm; 25 μ m Slit). Spectra are recorded during the arc using the spectrometer setup, which consists of a spectrometer connected to a computer through an optical fibre connection and connected to the deposition chamber on the opposite side. The resulting spectra can be analysed to determine temperature, density and other factors that influence the produced nanostructures, which are then investigated for morphological, elemental, and structural features.

Characterization. The excitation temperature and density within plasma are calculated using the Boltzmann plot method and the Saha-Eggert equation respectively (Safi *et al.*, 2019). The morphological, elemental and structural research is conducted by the SEM, EDX and XRD techniques respectively. We discuss all these characterizations in the following.

Excitation temperature measurement. The intensities of two consecutive spectral lines in the emission spectrum of the arc are plotted as a function of the time delay in the Fig. 2 which are used to estimate the excitation temperature and electron densities. The excitation temperatures are usually calculated with the help of the relative intensities of the spectral lines in the emission spectrum using the Boltzmann equation (Kolesnikov *et al.*, 2018) given below:

$$\ln[(\lambda_{ki}I)/(g_k A_{ki})] = C - [E_k/(k_B T)] \dots\dots\dots(1)$$

where:

I=relative intensity; λ_{ki} =wavelength; A_{ki} =transition probability; g_k =statistical weight of the upper level; E_k =energy of the upper level; k_B =Boltzmann's constant; T=excitation temperature. The values the transition probabilities, statistical weights and upper level's energies are obtained from the NIST database.

The excitation temperatures in the plasma arc can be found by using spectral lines in the emission spectrum

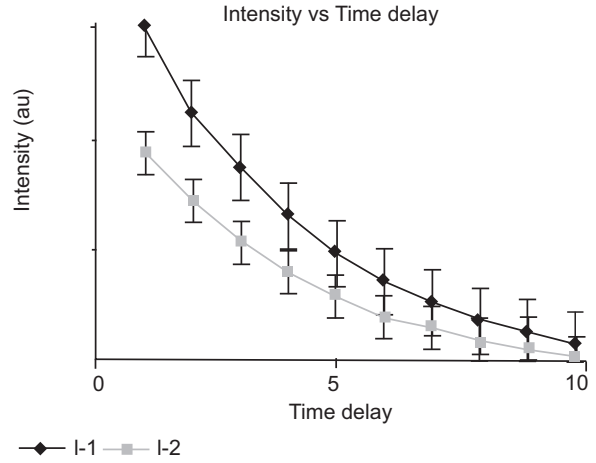


Fig. 2. The intensities of two consecutive spectral lines in the emission spectrum of the Arc are plotted as a function of the time delay which show the exponential behaviour.

of carbon. The Boltzmann function for different lines is calculated and plotted against the upper-level energy E_k as shown in the Fig. 3 and listed in the Table 1. The plot of Boltzmann function versus the energy of the upper level yields straight lines. The slopes (S) of these lines are $-1/k_B T$, assuming that there is a Boltzmann distribution in the population. We can write:

$$k_B T = -1/S \quad (\text{in eV}) \dots\dots\dots(2)$$

$$T = -[1/(k_B S)] \quad (\text{in K}) \dots\dots\dots(3)$$

Table 1 shows the electron temperatures obtained from the slopes of the Boltzmann plots of Fig. 3 which shows the drop from the maximum of 26650 $^{\circ}$ K to the minimum of 17777 $^{\circ}$ K during an interval of just 5 s. These measured values of are plotted as a function of delay time in the Fig. 4 which shows that the drop in the excitation temperature is exponential function of time.

Table 1. The measure values of the excitation temperature from the slopes of the Boltzmann plots of Fig. 3 are tabulated against the time delay

Time delay (ms)	Slope, S (eV) ⁻¹	$k_B T = -1/S$ (eV)	T (K)
1	-0.437	2.288	26550
2	-0.469	2.132	24744
3	-0.495	2.022	23468
4	-0.574	1.741	20203
5	-0.653	1.532	17777

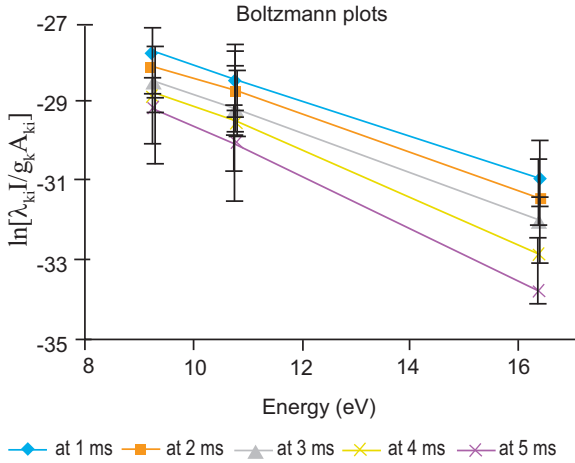


Fig. 3. Boltzmann function, $\ln[\lambda_{ki} I / g_k A_{ki}]$, plotted against the upper level energy (in eV) show the linear behaviour, the slopes of which can be used to find the excitation temperatures.

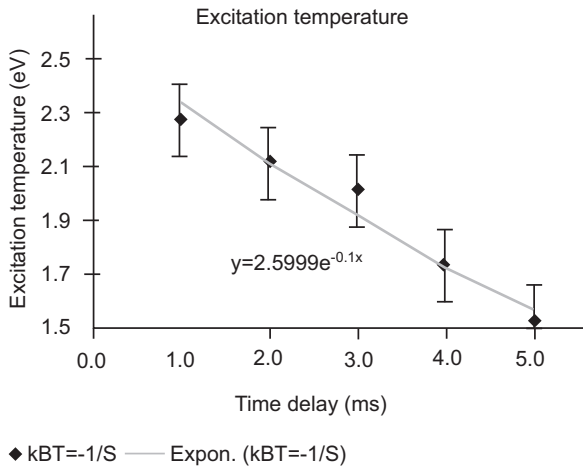


Fig. 4. The excitation temperature calculated from the Boltzmann plots of Fig. 3 are plotted as function of time delay. The exponential curve fit it is implied to find the dependance of excitation temperature on the time delay.

Electron density measurement. Saha-Eggert relationship is used to determine the electron density within plasma (Safi *et al.*, 2019). The relative intensities of the neutral atomic lines and the singly charged ionic lines of carbon are used in this equation.

$$N_e = 4.83 \times 10^{15} \left[\frac{I^{\circ} g^+ A^+ \lambda^{\circ}}{I^+ g^{\circ} A^{\circ} \lambda^+} \right] T^{3/2} \exp \left[\frac{E^+ + \Delta E_1 - E^{\circ} - E_1}{k_B T} \right] \dots \dots \dots (4)$$

where:

A° represent the neutral atom and the singly charged ion; I° is the relative emission intensity of the atomic line; I^+ is the relative emission intensity of the singly charged ionic line; E^+ is the energy of the excited state of the singly charged ions; E° is the energy of the excited state of the neutral atom; E_1 is the first ionization potential; ΔE_1 represents the lowering in the ionization potential which results from non-ideal plasma effects; T is the excited temperature; k_B is the Boltzmann's constant.

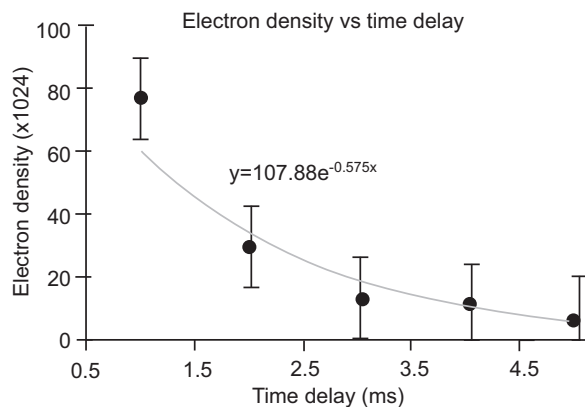
Table 2 shows the values of the transition probabilities, and the energies of upper levels for the carbon lines taken from the NIST database for the calculation of electron densities.

The estimated values of electron density versus delay time are plotted in the Fig. 5. The electron densities are also plotted against the excitation temperatures in Fig. 6. Figure 5 and Fig. 6 show that the dependence of electron density on both the delay time and excitation temperature is exponential.

Morphology. The nanotubes were deposited as soot on the cathode during the Arc. The soot is then collected from the cathode and analysed for the morphological and structural studies. The morphology of the nanotubes is studied by using the scanning electron microscopy (SEM). The scanning electron micrographs of the sample are shown in the Fig. 7 where the junks of carbon nanotubes can be seen. It can also be seen that the

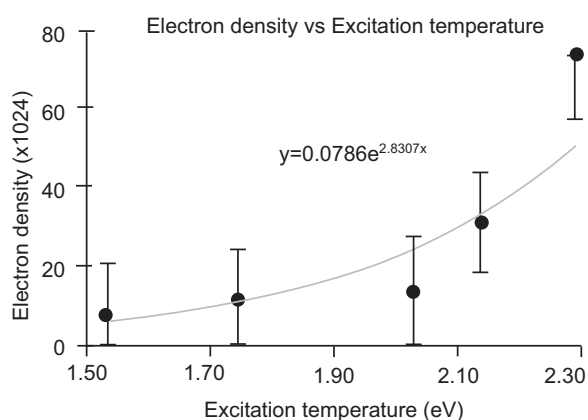
Table 2. The values of the transition probabilities and the energies of upper levels for the carbon lines taken from the NIST database to calculate electron densities

Wavelength λ (nm)	E_k (eV)	g_k	A_{ki} $\times 10^7/\text{cm}$	$\lambda_{ki}/g_k A_{ki}$ $\times 10^{14}$	$\ln[\lambda_{ki} I / g_k A_{ki}]$				
					at 0 ms	at 1 ms	at 2 ms	at 3 ms	at 4 ms
601.48	10.70	3	0.16	0.125	23.89	24.16	24.61	24.88	25.49
657.81	16.33	4	3.67	44.810	26.34	26.87	27.39	28.26	29.21
833.52	09.17	1	3.51	2.375	23.21	23.54	23.84	24.22	24.56



● Electron density

Fig. 5. Electron density of the plasma Arc, calculated from the Saha-Eggert equation, is plotted against the delay time, show the exponential decay as function of time.



● Electron density

Fig. 6. Dependence of the electron density on the excitation temperature. The graph shows that the electron density increases exponentially with increasing excitation temperature.

nanotubes formed during the DC Arc are of large lengths and very small in diameters. Additionally, it can also be seen in the SEM images that the orientation of nanotubes is completely random, as compared to parallel oriented nanotubes that can be formed by the method of chemical vapour deposition.

Composition. The elemental analysis of the samples is carried out by taking EDX spectra. Figure 8 shows the EDX spectrum of the sample. Purity index of the carbon

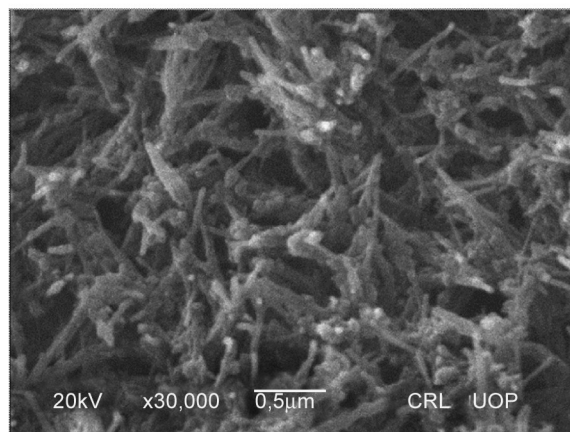
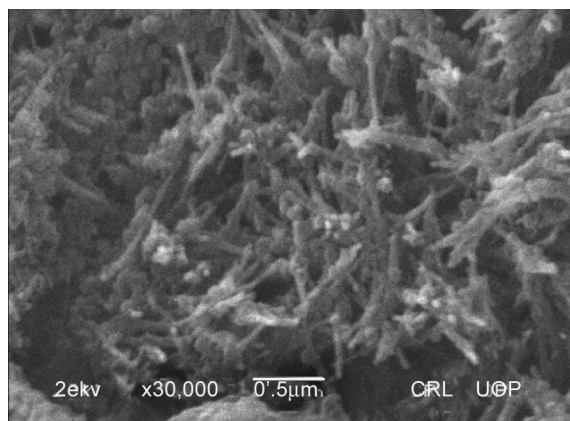


Fig. 7. SEM images of the sample showing nanotubes formed during the arc discharge. The junks of nanotubes can be seen here with large lengths and small diameters.

nanotubes is clear in the spectrum. There are three peaks in the spectrum. The most intense peak appeared at ~ 3 eV confirms that there are only carbon atoms present in the samples. The carbon is about 71% by weight and oxygen. It also proves the high purity of the graphite rods that are used as electrodes of the DC power supply for producing DC arc. The second peak is relatively very small, which shows the presence of oxygen atoms in the samples. This may be due to a little exposure of the samples with atmosphere. The third peak is gold, which is due to the fact that the samples were electroplated for SEM investigations.

Crystal structure. The XRD pattern of the sample is shown in Fig. 9 below:

The diffraction peaks appeared in the XRD spectrum match very well with the literature patterns. The most

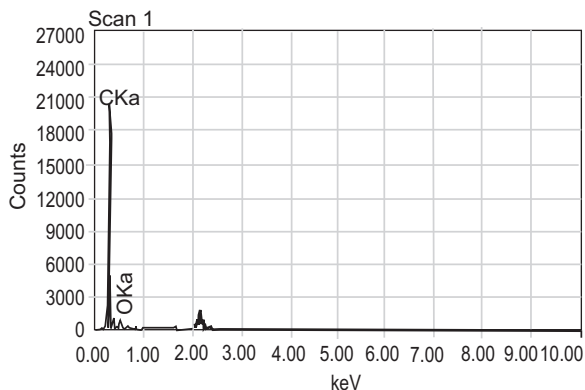


Fig. 8. EDX spectrum of the sample. The presence of the highest peak indicates the largest percentage of carbon present in the sample, whereas a very small peak of oxygen show very little content.

Table 3. The quantitative analysis of the samples performed using the EDX technique show the percent composition of the elements fitting coefficient: 0.9165

Element	(keV)	mass%	Error%	At%	K
C K	0.277	68.64	1.00	74.46	76.56
O K	0.525	31.36	8.15	25.54	23.43
Total		100.00		100.00	

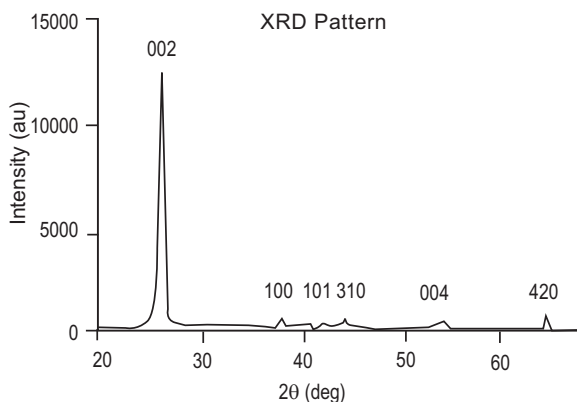


Fig. 9. XRD pattern of carbon nanotubes in which the intense peak at 26.4° shows the 002 reflection of the multiwalled carbon nanotubes. The other peaks at 42.4°, 44.55°, and 55° correspond to the 100, 101 and 004 reflections of the carbon atoms.

intense and sharp reflection peak (002) appeared at 26.4° indicates the concentric cylindrical nature of the graphene sheets nested together and that the nanotubes are multi-walled in nature (Mohamed *et al.*, 2015).

The presence of the peaks at 42.4° and 55° corresponding to the 100 reflections (Endo *et al.*, 1997) and 004 reflections (Boncel *et al.*, 2014) of carbon atoms respectively are also in good agreement with the literature (Endo *et al.*, 1997).

Plane Spacing. The planes’ spacing *d* for all peaks are calculated by using the Bragg’s law:

$$n\lambda = 2d \sin\theta \dots\dots\dots (6)$$

The calculated values of *d* are listed in Table 4. The most intense peak appeared at 26.4° in the XRD pattern confirms the presence of carbon nanotubes and the plane of this peak is named as 002 in the literature (Mohamed *et al.*, 2015; Gupta and Saleh, 2011; Liu *et al.*, 2008). The plane spacing at this peak is found to be 3.373 Å, which is also well matched with the literature for multi-walled carbon nanotubes (Dobrzanski *et al.*, 2010).

Table 4. Planes spacing for different peaks in XRD data of the carbon nanotubes are calculated by using the Bragg’s law

2θ (deg)	Intensity (I) (au)	I/I ₀ %	d-value (Å ⁰)
26.40	12278	100	3.373
38.25	540	4	2.352
42.40	345	3	2.130
44.55	655	5	2.032
64.90	641	5	1.436
69.30	236	2	1.355

Results and Discussion

During the evaporation of graphite rods, a portion of the positive electrode is consumed. The rate of reduction in the length of anode is measured to be 2 mm/s. Excitation temperatures are measured to be in the range of 20,000 to 30,000 °K that are in good agreement with the reported values (Harilal *et al.*, 1997). The electron densities in the arc plasma are measured to be of the order of x10²⁴ particles. In Fig. 5, the electron densities are falling exponentially with time, which in turn implies that the electron densities are decreasing exponentially with the decrease in temperature within the plasma.

The SEM images show that most of the particles have diameters ranging from approximately 5 to 30 nm and their lengths are of the order of hundreds of nanometres.

The EDX spectra of the samples shows the purity index of carbon in the prepared samples, which is found to be ~71 weight %. The second peak is relatively very small, which shows the presence of oxygen atoms in the samples. This may be due to a little exposure of the samples with atmosphere. The third peak (not labelled) is of gold, because the samples are electroplated with gold for the SEM/EDX analysis. The plane's spacing for 002 peak is calculated to be 3.373 Å by using Bragg's law.

Furthermore, the results are well matched with the literature patterns, according to which it is reported that the prepared nanostructures are multi-walled in nature (Mohamed *et al.*, 2015).

Conclusion

In this research, we have attempted to demonstrate some of the versatile capabilities of the small deposition chamber as a DC Arc system for the study of plasma during the processing of nanostructures. Multi-walled carbon nanotubes are successfully synthesized by this experimental setup. The excitation temperature and the density within the plasma are successfully calculated using the Boltzmann plots and the Saha-Eggert relationship, respectively. I have modified the system to control the temperature using water cooling and thermostat to enhance its performance for a variety of depositions for future work. This system is very flexible that allows the deposition of various materials with a very less mechanical job and in a very short span of time (within few minutes if working at room temperature). The viewing window is positioned vertically to the plasma column, making the setup very appropriate to scan the plasma for spectroscopic studies. In conclusion, such setup is very useful to find quick results as far as characterization is concerned.

Conflict of Interest: The authors declare that they have no conflict of interest.

References

Aabir, A., Naz, M.Y., Shukrullah, S. 2022. Synthesis of carbon nanotubes *via* plasma arc discharge method. In: *Emerging Developments and Applications of Low Temperature Plasma*, pp. 85-102, IGI Global.

- Arora, N., Sharma, N.N. 2014. Arc discharge synthesis of carbon nanotubes: comprehensive review. *Diamond and Related Materials*, **50**: 135-150.
- Bethune, D.S., Kiang, C.H., De Vries, M.S., Gorman, G., Savoy, R., Vazquez, J., Beyers, R. 1993. Cobalt catalysed growth of carbon nanotubes with single atomic layer walls. *Nature*, **363**: 605-607.
- Boncel, S., Pattinson, S.W., Geiser, V., Shaffer, M.S., Koziol, K.K. 2014. An route to controlled catalytic CVD synthesis of densely packed and vertically aligned nitrogen-doped carbon nanotube arrays. *Beilstein Journal of Nanotechnology*, **5**: 219-233.
- Collins, P.G., Avouris, P. 2000. Nanotubes for electronics. *Scientific American*, **283**: 62-69.
- Dobrzanski, L.A., Pawlyta, M., Krztoń, A., Liszka, B., Labisz, K. 2010. Synthesis and characterization of carbon nanotubes decorated with platinum nanoparticles. *Journal of Achievements in Materials and Manufacturing Engineering*, **39**: 184-189.
- Endo, M., Takeuchi, K., Hiraoka, T., Furuta, T., Kasai, T., Sun, X., Kiang, C.H., Dresselhaus, M.S. 1997. Stacking nature of graphene layers in carbon nanotubes and nanofibres. *Journal of Physics and Chemistry of Solids*, **58**: 1707-1712.
- Gupta, V., Saleh, T.A. 2011. Syntheses of carbon nanotube metal oxides composites; adsorption and photo-degradation. *Carbon Nanotubes-From Research to Applications*, **17**: 295-312.
- Harilal, S.S., Bindhu, C.V., Issac, R.C., Nampoori, V.P.N., Vallabhan, C.P.G. 1997. Electron density and temperature measurements in a laser produced carbon plasma. *Journal of Applied Physics*, **82**: 2140-2146.
- Iijima, S. 1991. Helical microtubules of graphitic carbon. *Nature*, **354**: 56-58.
- Iijima, S., Ichihashi, T. 1993. Single-shell carbon nanotubes of 1-nm diameter. *Nature*, **363**: 603.
- Kolesnikov, I.E., Kurochkin, M.A., Kalinichev, A.A., Kolesnikov, E.Y., Lähderanta, E. 2018. Optical temperature sensing in Tm³⁺/Yb³⁺-doped GeO₂-PbO-PbF₂ glass ceramics based on ratiometric and spectral line position approaches. *Sensors and Actuators A: Physical*, **284**: 251-259.
- Krätschmer, W., Lamb, L.D., Fostiropoulos, K.H.D.R., Huffman, D.R. 1990. Solid C60: a new form of carbon. *Nature*, **347**: 354-358.
- Liu, G., Zhao, Y., Zheng, K., Liu, Z., Ma, W., Ren, Y., Xie, S., Sun, L. 2009. Coulomb explosion: a novel approach to separate single-walled carbon nanotubes from their bundle. *Nano Letters*, **9**: 239-244.

- Mohamed, A., Osman, T.A., Khattab, A., Zaki, M. 2015. Tribological behavior of carbon nanotubes as an additive on lithium grease. *Journal of Tribology*, **137**.
- Phys.org, 2012. New Technique Connects Multi-walled Carbon Nanotubes (A Method), Georgia Institute of Technology, (2012, October 30) Retrieved May 22, 2023 from <https://phys.org/news/2012-10-technique-multi-walled-carbon-nanotubes.html>
- Safi, A., Tavassoli, S.H., Cristoforetti, G., Legnaioli, S., Palleschi, V., Rezaei, F., Tognoni, E. 2019. Determination of excitation temperature in laser-induced plasmas using columnar density Saha-Boltzmann plot. *Journal of Advanced Research*, **18**: 1-7.
- Saito, Y., Inagaki, M., Shinohara, H., Nagashima, H., Ohkohchi, M., Ando, Y. 1992. Yield of fullerenes generated by contact arc method under He and Ar: dependence on gas pressure. *Chemical Physics Letters*, **200**: 643-648.
- Watanabe, T. 2013. Innovative thermal plasma processing from fundamental research. In: *Proceeding of 21st International Symposium on Plasma Chemistry (ISPC 21)*, August 4-9, 2013, 4 pp., Cairns Convention Centre, Queensland, Australia.